Central Mindanao University
Journal of Science
ISSN Print: 0116-7847 ISSN Online: 2704-3703

GIS-based Mapping of Flashflood Susceptible Areas in Bukang Liwayway, Kibawe, Bukidnon

George R. Puno, Alex S. Olpenda, Rena Christina C. Puno, Rodriga G. Aguinsatan, Laarni F. Lacandula, Ida V. Maghuyop, and Ricardo G. Villar

College of Forestry and Environmental Science
Central Mindanao University, Musuan, Bukidnon, Philippines, 8710

ABSTRACT

This study aimed to generate a GIS-based flashflood hazard susceptibility map using the geographical information system (GIS) and frequency ratio (FR) techniques in one of the geographically isolated and disadvantaged areas (GIDAs) of the country, which is the barangay Bukang Liwayway of Kibawe, Bukidnon. There are 160 sample points conducted for flashflood inventory to calculate FR and the flashflood prediction weights values needed to generate the flashflood susceptibility map. The elevation, slope, aspect, curvature, topographic wetness index, drainage density, LULC, normalized difference vegetation index, and rainfall are the nine controlling factors that are selected. Results show that the areas exposed to flashflood with low, medium, and high-risk levels of susceptibility consist of 89.8, 4.4, and 5.7% of the total land, respectively, with 25 households exposed to high risk. The study determined the possible site for the evacuation center based on the spatial analysis resulting in the overlaying of different thematic map layers based on flashflood susceptibility factors. The study emphasizes the integration of the findings in the localized comprehensive land-use plan to realize the challenge of building a sustainable and hazard-resilient human community in Bukang Liwayway.

Keywords: Flashflood-resilient, frequency ratio, GIDAs, GIS, susceptibility

INTRODUCTION

Climate change-related hazards like floods, landslides, and soil erosion are common in tropical countries like the Philippines. The topographic characteristics in most highlands of the country, like Bukang Liwayway, Kibawe, Bukidnon, typically result in high-intensity rainfall. With the uncontrolled land tilling in steeper hillslopes and other anthropogenic factors, the area is prone to accelerated soil erosion and, to some extent, heightened exposure to landslide and flood hazards. In most cases, these areas are confronted primarily with the problems such as soil erosion and sedimentation, disturbed riparian areas, and low water quality. With the degrading soil and water resources, farmers tend to move into areas with fertile soil in the uplands resulting in land conversion for crop production, which depletes the remaining natural forest resources. Continued degradation of soil, water, and forest resources may negatively affect the income of individual households and the local economy of Bukang Liwayway.

According to the Central Mindanao University Integrated Research Development and Extension (CMU iRDE) Program "Capacitate" Project teams' exploration and needs assessment, Bukang Liwayway is confronted primarily with the issues and concerns relative to income, natural resources, and hazards. Some of these include lack of potable water, low income from corn production, lack of other sources of livelihood, soil and water degradation, and lack of land use/land cover (LULC) maps and hazard maps.

The aim of this research project had focused on generating a GIS-based map of hazards and natural resources like forest vegetation of the study area. The study recognizes the advantage of using the Geographic Information System (GIS) and the need for integrating modern technology and indigenous knowledge into disaster management (Tran et al., 2009). The project mobilizes human and technical resources to strengthen a good partnership between local communities and government institutions like CMU. Generally, the project provides information to local government units to aid in legislating policies and ordinances relative to flood hazard reduction and management. The LGU can use the output of this study to establish linkages with the national and international agencies to support the implementation of programs and projects on disaster risk reduction and mitigation.

METHODOLOGY

Description of the study area

The study area is located in Barangay Bukang Liwayway with a geographical extent of 7^0 28′ 20″ to 7^0 30′ 23″ North and 125^0 0′ 44″ to 125^0 2′ 17″ East (Figure 1). Within the Municipality of Kibawe, Province of Bukidnon, Bukang Liwayway is constituted with seven Puroks and identified as one of the country's geographically isolated and disadvantaged areas (GIDAs). It has an approximate area of 623.23 hectares with 307 households. Bukang Liwayway is bounded by the barangays of Balintawak at the North, Cagawasan and Sampaguita at the East, Sanipon at the South, Mascariñas and Tumaras at the West.

Corresponding author:
George R. Puno
Email Address: grpuno@cmu.edu.ph
Received: Feb. 21, 2022; Accepted: Jun. 29, 2022

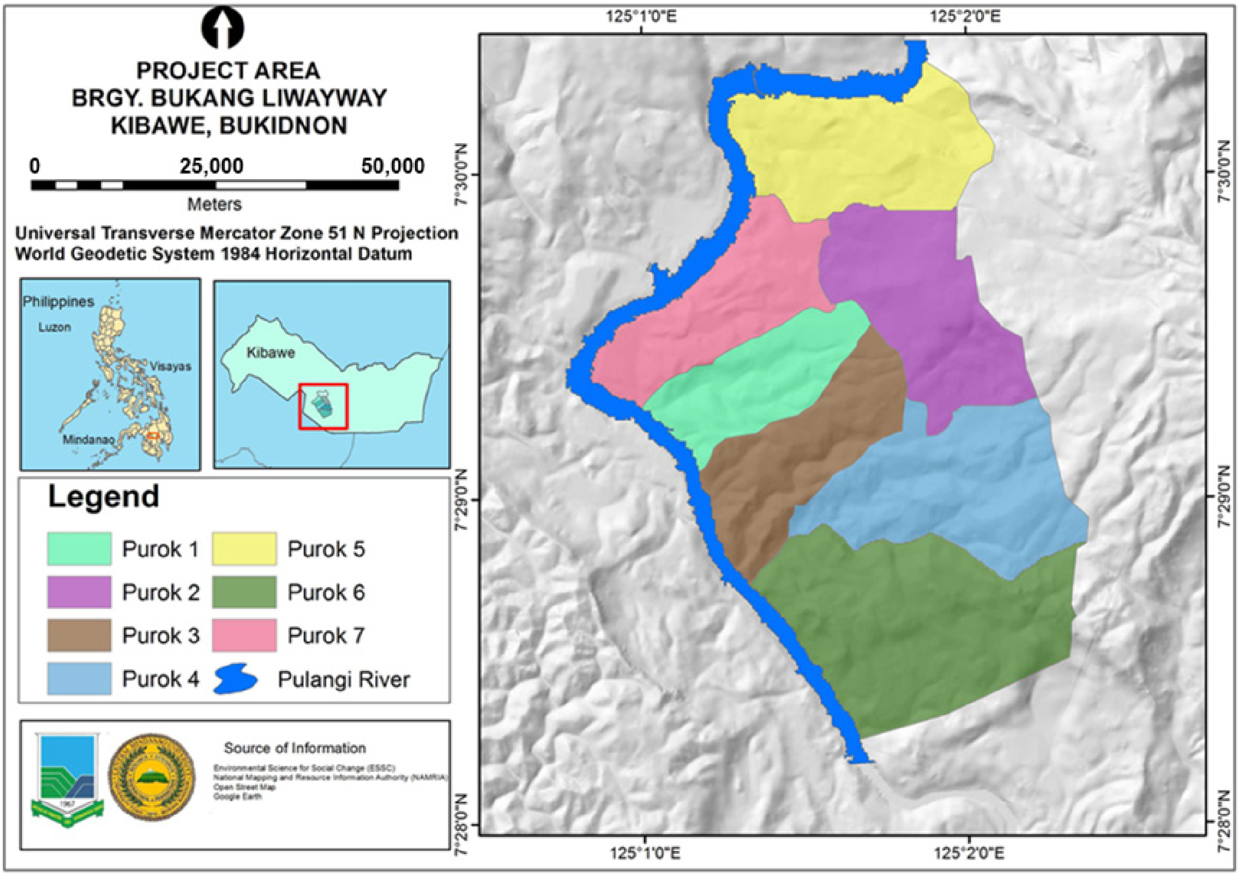

Figure 1. Map of Bukang Liwayway, Kibawe, Bukidnon

The barangays of Balintawak, Tumaras, and Mascariñas is demarcated from barangay Bukang Liwayway as the Pulangi River traverses from the North to South on the western side.

The area's topography is mostly rolling based on the average slope of 31%, with the lowest and the highest elevations of 64 and 407 meters above sea level (masl). The area's climate belongs to type four with no distinct dry season and an annual precipitation average of 2,800 mm. The vegetations are mainly agricultural, with patches of primary and secondary forest.

Data Collection and Processing

Mapping flash flood hazards need four essential input files: climate, slope, soils, and land cover. These input files could either be primary or secondary data. Primary data gathering includes the collection of coordinates using a global positioning system (GPS) from the sample points on the ground with flood incidences and the LULC map of 2021 generated using a Sentinel-2 satellite image.

The 2021 Sentinel-2 satellite image product was downloaded from the internet through the United States Geological Survey (USGS) Earth Explorer. The image was processed using a remote sensing tool to generate a vector map layer for the LULC of the area. The method included the collection of the training samples which were used to perform the maximum likelihood classification algorithm. The next phase consisted of collection validation sample points of different land cover classes on the ground, independent from the training samples based on the image from google earth aerial photos. The process applied the confusion matrix analysis to obtain the producer, user, and overall accuracy values. The producer accuracy refers to the probability that a particular land cover class is classified as such, while the use accuracy refers to the likelihood of the same identity between a pixel and the actual land class in the map (Rwanga and Ndambuki, 2017. LULC classification produces several features where some are irrelevant in the map layout. Thus, the process applied the minimum likelihood unit tool to decongest the map from unnecessary segmented polygons.

The visual observation was conducted to assess the area's environmental conditions and characteristics, including the vegetation around the flooded areas. An inventory of past flashfloods incidence was conducted to generate the database comprising the relationship between the different triggering factors and flood occurrences. In the study, the flood database was created based on the collected coordinates of the 160 flood points using GPS.

The secondary data collected includes the interferometric synthetic aperture radar (IFSAR) from the National Mapping and Resource Information Authority (NAMRIA) to generate Digital Elevation Model (DEM), satellite images obtained from the United States Geological Survey (USGS) earth explorer for the land cover, and the historical rainfall of the Philippine Atmospheric, Geophysical, and Astronomical Services Administration (PAGASA) weather stations. Figure 2 shows the process flow chart of the study following the method employed by Ullah and Zhang (2020).

All flashflood controlling factors were reclassified into an appropriate number of values. This work conducted

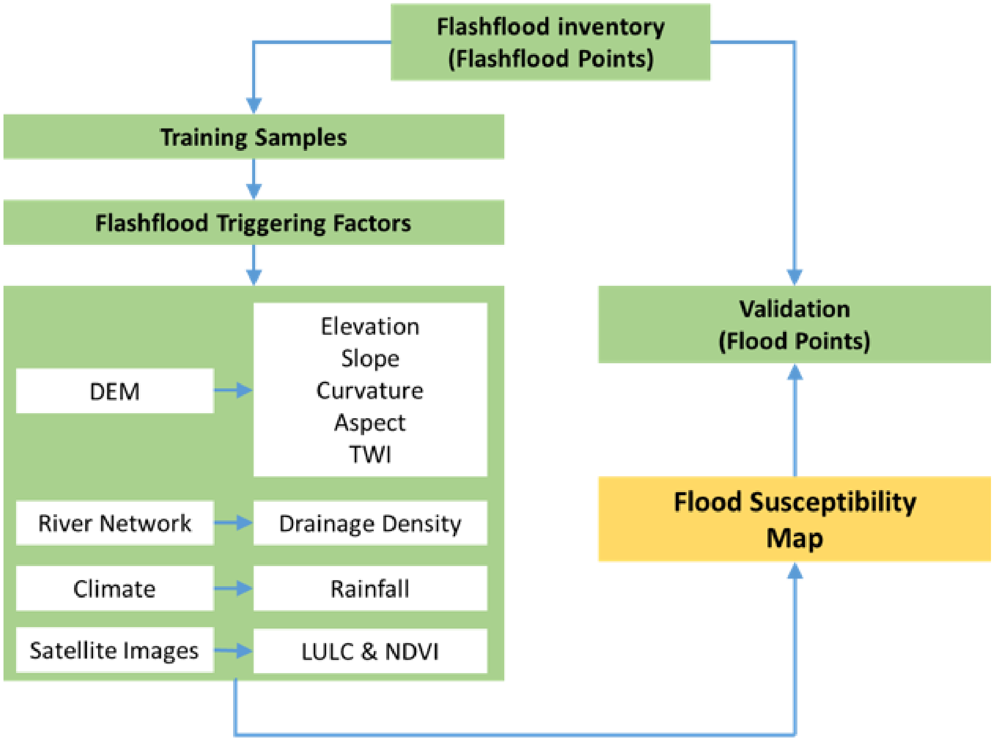

Figure 2. Process flow chart of mapping the flashflood susceptible areas

manual classification with discrete classes for the factors with continuous values. Following the GIS workflows, the generated datasets were converted into raster format with the same geographic projection and resolution. The correlation between flash flood susceptibility controlling factors and flashflood inventory was analyzed by frequency ratio and flashflood relative frequency ratio.

Relative Frequency Ratio in Flashflood Susceptibility Mapping

Any area's flash flood hazard susceptibility can be estimated based on the contribution of causative factors and the relationship between them. With the advent of powerful computers, machine learning methods are widely used. However, these methods require a massive amount of data as training for better accuracy (Acharya and Lee, 2018). Due to the limited data and the corresponding cost constraint, this study used the relative frequency ratio (FR) method of flashfloods susceptibility mapping in different controlling factors within the GIS platform. FR is based on the observed relationship between the spatial distribution and causative factors of flashflood susceptibility such as elevation, slope, aspect, curvature, TWI, drainage density, LULC, NDVI, and rainfall expressed mathematically as:
The FR values were normalized in a range of probability

$$\text{Eq. 1} \qquad FR = \frac{Flood\ points\ in\ factor\ calss \,/\, Total\ flashflood\ points}{Factor\ clas\ area \,/\, Total\ factor\ class\ area}$$

values (0, 1) a Relative Frequency (RF). The RF for each class were calculated using the following equation:

$$\text{Eq. 2} \qquad RF = \frac{Factor\ class\ FR}{\sum Factor\ classes\ FR}$$

After the normalization, the RF values still have the drawback of considering all conditioning factors equal weight. For the purpose to address the drawback and considering the mutual interrelationship among the independent variables, prediction rate (PR) was calculated for the rating of every conditioning factor with the training datasets as:

$$\text{Eq. 3} \qquad PR = \frac{RF_{max} - FR_{min}}{(RF_{max} - RF_{min})_{min}}$$

Finally, the flash flood susceptibility index map (FSI) was calculated by the summation of the product of each factor PR and each class of the maximum normalized FR values as shown below:

$$\text{Eq. 4} \qquad FSI = \sum_{i=1}^{n} PR_i (RF_i)$$

Validation was made through visual observation in the area with the residents to confirm the actual occurrence of the flash flood hazards.

Data Analysis and Validation

Descriptive analysis such as total, mean, and percentage was applied to describe the extent of the different controlling factors and the resulting simulated flashflood susceptible areas. Geospatial analysis such as spatial join, intersect, overlay, etc., within the GIS platform was also conducted to determine the results of the combined thematic map layers of interest. Validation was conducted through an actual field survey with the presence of localities to confirm the location of flashflood occurrence. Sample points were collected and used to attest to the validity of the simulated flash flood hazards.

RESULTS AND DISCUSSION

There were nine triggering factors of flashflood hazards included in the study, namely: elevation, slope, aspect, curvature, TWI, drainage density, Land use/Land cover change (LULC), Normalized difference vegetation index (NDVI), and rainfall. Figure 3 shows the different GIS map layers of the selected triggering factors for flashflood susceptibility mapping of Bukang Liwayway. The topographic features of the barangay in terms of elevation and slope are visualized in Figures 3a and 3b, respectively. Lower elevated areas are mostly planted with different crops, while the higher elevated areas are covered with isolated forest patches and farming crops. Built-ups or residential areas are usually situated at the mid-elevation range of 210 to 260 masl. The elevation class of 113-150 masl constitutes the most extensive (22.63%) of the total area of the barangay (Table 1). The mid-elevation with 12.84% of the total area is of particular interest as flood peaks for a given return period of rainfall events also increase with mean watershed elevation (Dingman, 1981). However, this has yet to be further validated as the study area was delineated as not following the watershed natural boundary.

Accordingly, elevation and slope are the important factors of flashflood occurrence as water always flows from higher locations to low-lying areas. The lowest elevation class (64-112 masl) has the maximum RF value of 0.56, followed by 113-150, 189-230, 151-188, and 231-407 masl with FR values of 0.308, 0.07, 0.06 and 0, respectively. The analysis reveals that flashflood occurrences are mostly in the lower elevation class. Higher elevation classes have the lowest FR value (Table 2). These results agree with previous studies, which found a low probability of flood occurrences at higher elevated regions and a high probability of flooding in lowland areas (Ullah and Zhang, 2020).

The area's slope was classified in accordance to the Bureau of Soil and Water Management (BSWM) slope categories described as flat (0-3%), undulating (3.01-8%), undulating to rolling (8.01-18), rolling (18.01-30%), steep (30.01-50%), and very steep (>50%). Accordingly, the relative slope length factor has also been considered one of the fundamental causes that contribute to flood hazards and can prove the existence of a strong relationship between flooding and flat areas of low elevation (Nguyen et al., 2020; Tehrany et al., 2017). The infiltration process is also partly controlled by the slope gradient. An increasing gradient decreases the infiltration process but increases the surface runoff; as a result, in regions having a sudden descent gradient, an enormous extent of water becomes stagnant and causes flood conditions (Ullah and Zhang, 2020). The average slope of the barangay falls under the slope category of rolling, with an average of 31%. The results show that the two lower slope gradient classes, i.e., less than 3 and 4-8 % have the highest FR value of 0.335 and 0.313, respectively. In contrast, the slope gradients above 50 % show the lowest RF value (Table 2).

Meanwhile, the aspect or exposure of the barangay (Figure 3c) is mostly southwest, covering 43.14% of the area. As reported, southwest orientation exposure has a high tendency to be susceptible to flash floods due to poor vegetation cover and dry ground surface (Avinash and Ashamanjari, 2010). The aspect was selected for this analysis due to its impact on the amount of precipitation and sunlight exposure (Tehrany et al., 2017). Excluding flat, all other classes of this factor exhibited a relationship with flooding, with the strongest found at the southwest. The barangay is unique from other places in terms of curvature as it has a minimal flat surface. As shown in Figure 3d, the curvature map classifies into three classes: concave upward for negative values, flat for zero values, and convex upward for positive values. The result shows that the highest RF was obtained from the surface with concave curvature, indicating that flashflood usually occurs in these areas.

The topographic wetness index (TWI) map of the site, classified into five different classes (Figure 3e), shows that most of the area (40.56%) has a lower TWI value indicating that only a lesser portion of the area is susceptible to flashflood. The location is usually near the creeks. Around 11.22% of the area with TWI ranging from 6.9 to 18.4 is more susceptible to flooding.

The drainage density of Bukang Liwayway (Figure 3f) was classified into five classes for visualization. The map shows that higher drainage densities are concentrated in the small proportion of the area along the streamlines towards the Pulangi River. High drainage density scattered near the Pulangi River indicates high groundwater occurrence and surface runoff; and, therefore, favors a high probability of flooding. It is considered that drainage density is an essential factor having a direct relationship with flooding (Ullah and Zhang, 2020). An area with low drainage density causes more infiltration and decreased surface runoff and is suitable for groundwater development (Dinesh Kumar et al., 2007).

On the other hand, the LULC of the barangay, classified into different types, is shown in Figure 3g. The categories identified include built-up, forest, mixed vegetation, water, perennial and seasonal crops. The perennial crops are the coconut, rubber, and plantation trees while the seasonal crops are the agricultural ones such as corn and other cash crops. Mixed vegetation is the intercropped of different plants which dominate the area covering 49.55% of the barangay. The seasonal crop is the second largest LULC with 27.12% cultivated for agricultural production. As a common observation, the rolling terrain of the barangay with unprescribed cultivation makes it more prone to flashflood and other natural hazards.

Another controlling factor considered in this study is the normalized difference vegetation index (NDVI). Figure 3h shows the generated NDVI of the area. This measures surface reflectance and quantify vegetation growth and biomass (Wu, Li, Wang, & Yan, 2016). This study classified the NDVI map into three classes to represent the different degrees of vegetation density with the lower and higher values for barren and vegetated lands, respectively. NDVI has a negative relationship with flooding, having a value range of -1 to +1. Higher NDVI values indicate lower susceptibility to flooding, and lower NDVI values indicate higher flood probability (Ullah and Zhang, 2020). In this study, however, the NDVI values range from -0.12 to 0.80 failed to prove the stated relationship maybe because of some controlling factors that the study has missed to consider.

Meanwhile, the annual rainfall map, classified into five different classes, is shown in Figure 3i. The demarcation of rainfall values into different classes determines the

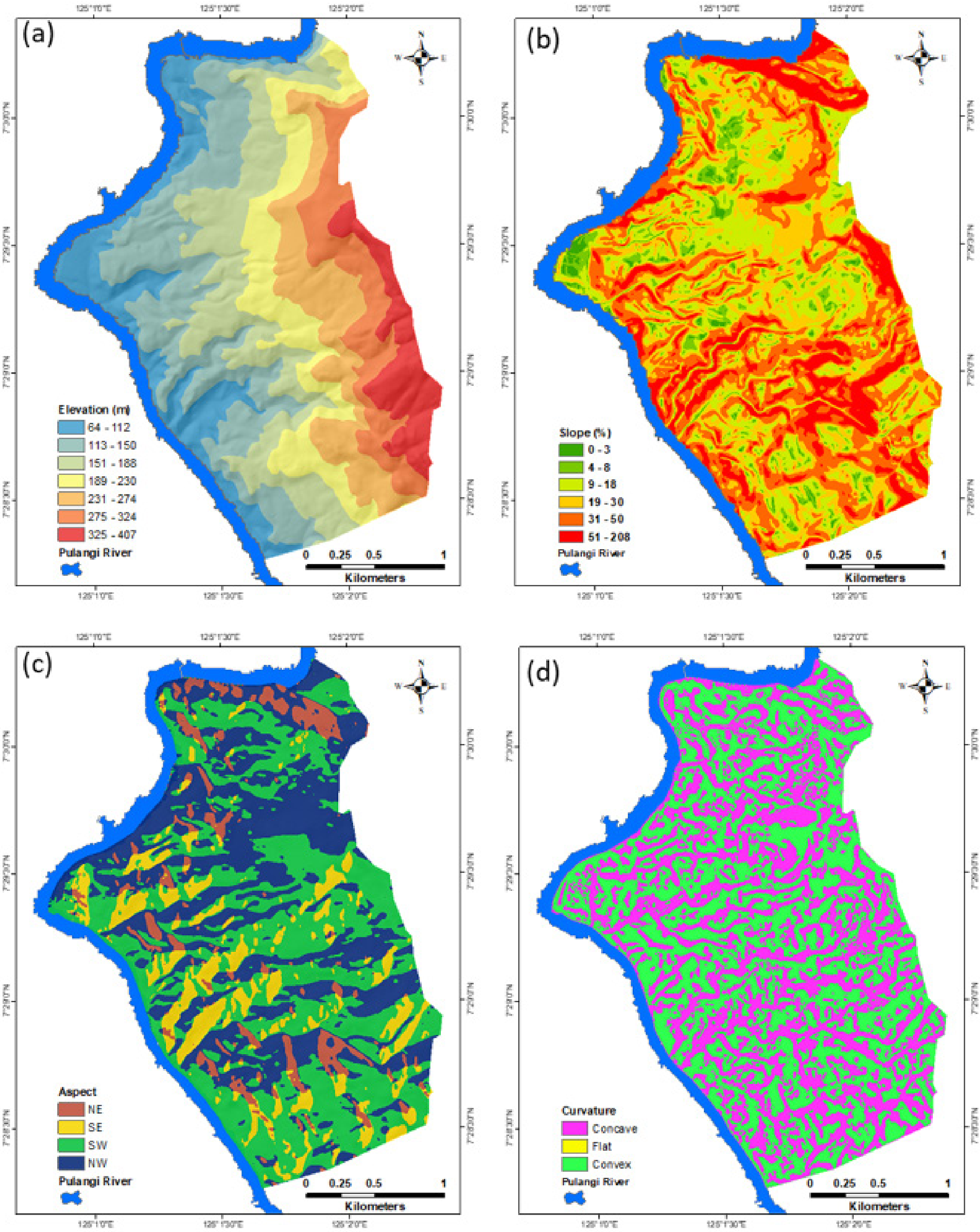

Figure 3. Triggering factors of flashflood hazard; (a) elevation, (b) slope, (c) aspect, (d) curvature

effect of rainfall amount to flash flood events in different locations. The highest rainfall is at the eastern part of the barangay with higher elevations. The rainfall pouring in these areas generates surface runoff that flows towards the Pulangi River, where most flash flood events occur. Accordingly, rainfall directly relates to river discharge, and a large amount of rain in a short time can generate flashflood in semiarid regions (Ullah and Zhang, 2020). The spatial analysis shows that the highest RF falls within the areas with lower rainfall amounts. However, the flash flood that occurred in these areas resulted from the accumulated rainwater from higher elevated regions that received a greater amount of rainfall.

Flashflood Susceptibility Map

After preparing the nine map layers of the flashflood controlling factors and giving weights of each parameter using the FR and RF method, a final flashflood hazard map was generated by the summation of each factor prediction rate and each class RF in a raster calculator of the ArcGIS 10.3 software. The flash flood susceptibility index map of Bukang Liwayway, classified into three levels of risk (low, medium, high), is shown in Figure 4. Results show that the areas exposed to flashflood with low, medium, and high-risk levels of susceptibility consist of 89.8, 4.4, and 5.7% of the total land, respectively. As shown in the FSI map, areas with higher levels of flashflood susceptibility, depicted

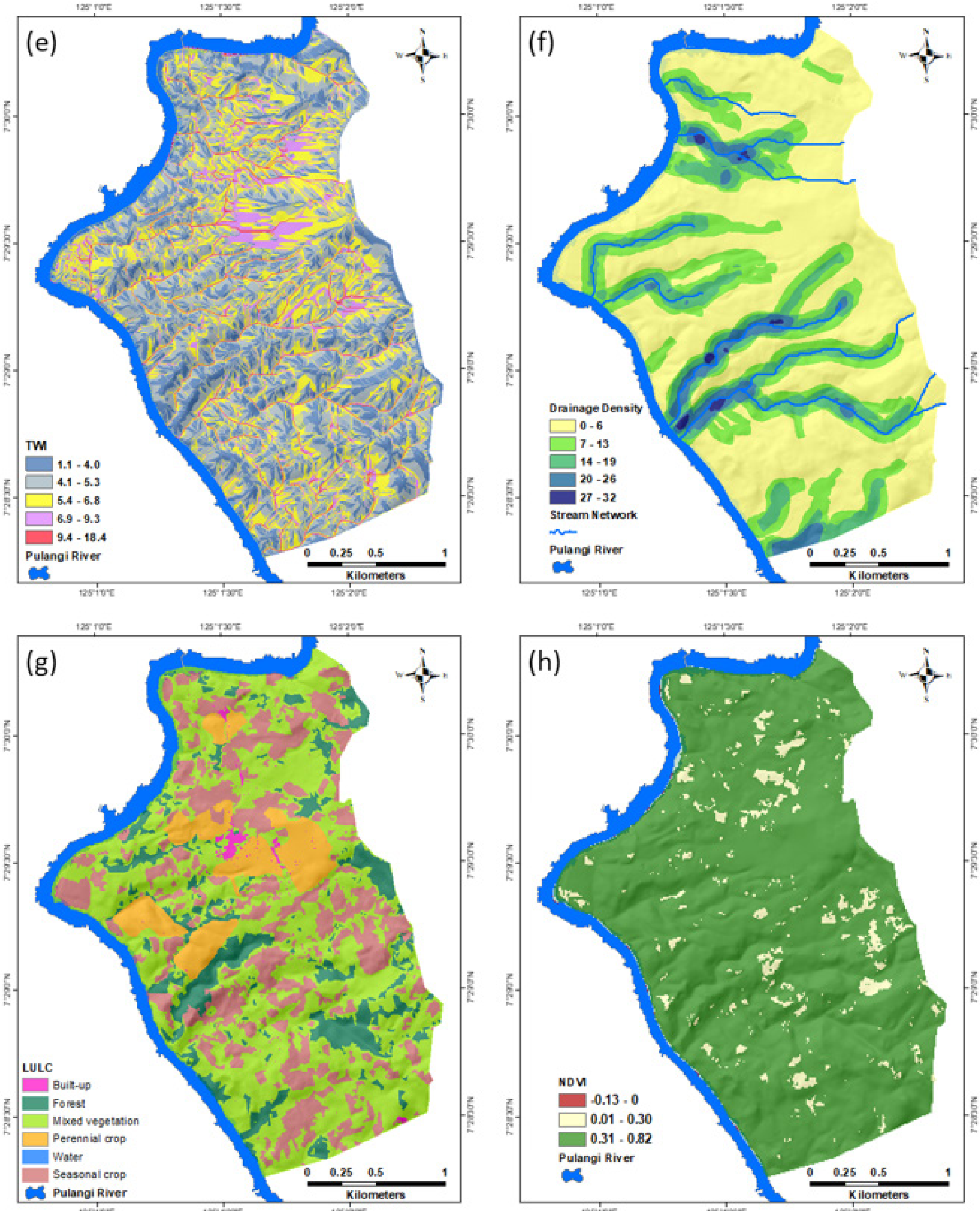

Figure 3. (continued).. (e) TWI, (f) drainage density, (g) LULC, (h) NDVI

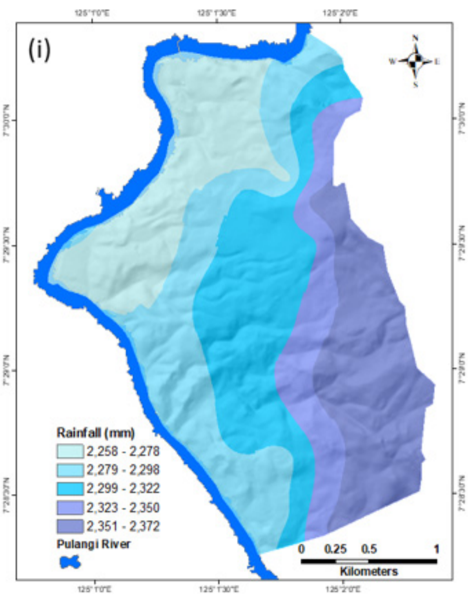

Figure 3. (continued).. (i) rainfall.

Table 1. Frequency ratio and relative frequency for all classes of factors.

Factors	Factor Classes (a)	Sample Points (b)	% of Points (c)	Class Area (d)	% of Area (e)	FR (c/e)	RF
Elevation	64-112	80	50.00	99.93	16.03	3.12	0.561
	113-150	62	38.75	141.02	22.63	1.71	0.308
	151-188	10	6.25	116.35	18.67	0.33	0.060
	189-230	8	5.00	80.05	12.84	0.39	0.070
	231-274	0	0.00	79.37	12.74	0.00	0.000
	275-324	0	0.00	61.42	9.86	0.00	0.000
	325-407	0	0.00	45.06	7.23	0.00	0.000
Slope	0-3	7	4.38	8.89	1.43	3.07	0.335
	4-8	27	16.88	36.67	5.88	2.87	0.313
	9-18	44	27.50	131.94	21.17	1.30	0.142
	19-30	46	28.75	164.35	26.37	1.09	0.119
	31-50	33	20.63	180.32	28.93	0.71	0.078
	51-208	3	1.88	101.04	16.21	0.12	0.013
Aspect	NE	13	8.13	45.205	7.25	1.12	0.219
	SE	48	30.00	76.94	12.35	2.43	0.476
	SW	45	28.13	268.83	43.14	0.65	0.128
	NW	54	33.75	232.24	37.26	0.91	0.177
Curvature	Concave	144	90.00	292.5	46.93	1.92	0.911
	Flat	0	0.00	0	0.00	0.00	0.000
	Convex	16	10.00	330.72	53.07	0.19	0.089
TWI	1.01-4.0	10	6.25	139.54	22.39	0.28	0.018
	4.1-5.3	36	22.50	252.76	40.56	0.55	0.035
	5.4-6.8	42	26.25	161.03	25.84	1.02	0.064
	6.9-9.3	22	13.75	54.27	8.71	1.58	0.099
	9.4-18.4	50	31.25	15.62	2.51	12.47	0.784
Drainage density	0 – 6	6	3.75	372.99	59.85	0.06	0.005
	7 – 13	7	4.38	127.88	20.52	0.21	0.016
	14 – 19	78	48.75	90.64	14.54	3.35	0.258
	20 – 26	69	43.13	28.66	4.60	9.38	0.721
	27 - 32	0	0.00	3.05	0.49	0.00	0.000
LULC	Built-up	0	0.00	5.00	0.80	0.00	0.000
	Forest	49	30.63	79.81	12.81	2.39	0.454
	Mixed vegetation	66	41.25	308.78	49.55	0.83	0.158
	Perennial crop	23	14.38	58.22	9.34	1.54	0.292
	Water	0	0.00	2.41	0.39	0.00	0.000
	Seasonal crop	22	13.75	169.01	27.12	0.51	0.096
NDVI	<0	0	0.00	0.39	0.06	0.00	0.000
	0.01 – 0.30	0	0.00	38.71	6.21	0.00	0.000
	>0.30	160	100.00	584.34	93.76	1.07	1.000
Rainfall	2,258 – 2,278	40	25.00	128.44	20.61	1.21	0.514
	2,279 – 2,298	20	12.50	146.14	23.45	0.53	0.226
	2,299 – 2,322	17	10.63	148.98	23.90	0.44	0.188
	2.323 – 2,350	3	1.88	69.54	11.16	0.17	0.071
	2,351 – 2,372	0	0.00	130.07	20.87	0.00	0.000

with red, are concentered in the lower elevated areas with higher drainage densities. Similarly, Figure 5 shows the FSI map overlaid with the household and the road network map layers. This method allows determining the number of households at risk of a high level of flash flood hazard and the possible site for the evacuation center. Based on spatial analysis, 25 and 22 households in the barangay are exposed to high and medium levels of flashflood susceptibility, respectively (Figure 6). Areas with high flashflood susceptibility are mostly observed near the river banks particularly those with steeper slopes. Moreover, the soil properties particularly its texture are observed to be composed of loose particles and mostly sandy which makes it more prone to rainfall-induced landslide. The spatial distribution of flashflood susceptibility generated in this study is very helpful information in crafting a policy for risk reduction and mitigation thereby minimizing the impact of flashflood hazards in the affected communities. The recommended site for the evacuation center (Figure 5) is approximately 60 meters away from the barangay road making it readily accessible when a disaster occurs. The terrain is undulating to rolling with an average elevation of

Table 2. Weights of evidence or prediction rate for all conditioning factors.

Factors	Relative Frequency (min)	Relative Frequency (max)	Relative Frequency (max-min)	Prediction Rate (PR)
Elevation	0.00	0.56	0.561	1.74
Slope	0.01	0.34	0.322	1.00
Aspect	0.13	0.48	0.348	1.08
Curvature	0.00	0.91	0.911	2.83
TWI	0.02	0.78	0.766	2.38
Drainage density	0.00	0.72	0.721	2.24
LULC	0.00	0.45	0.454	1.41
NDVI	0.00	1.00	1.000	3.11
Rainfall	0.00	0.51	0.514	1.60

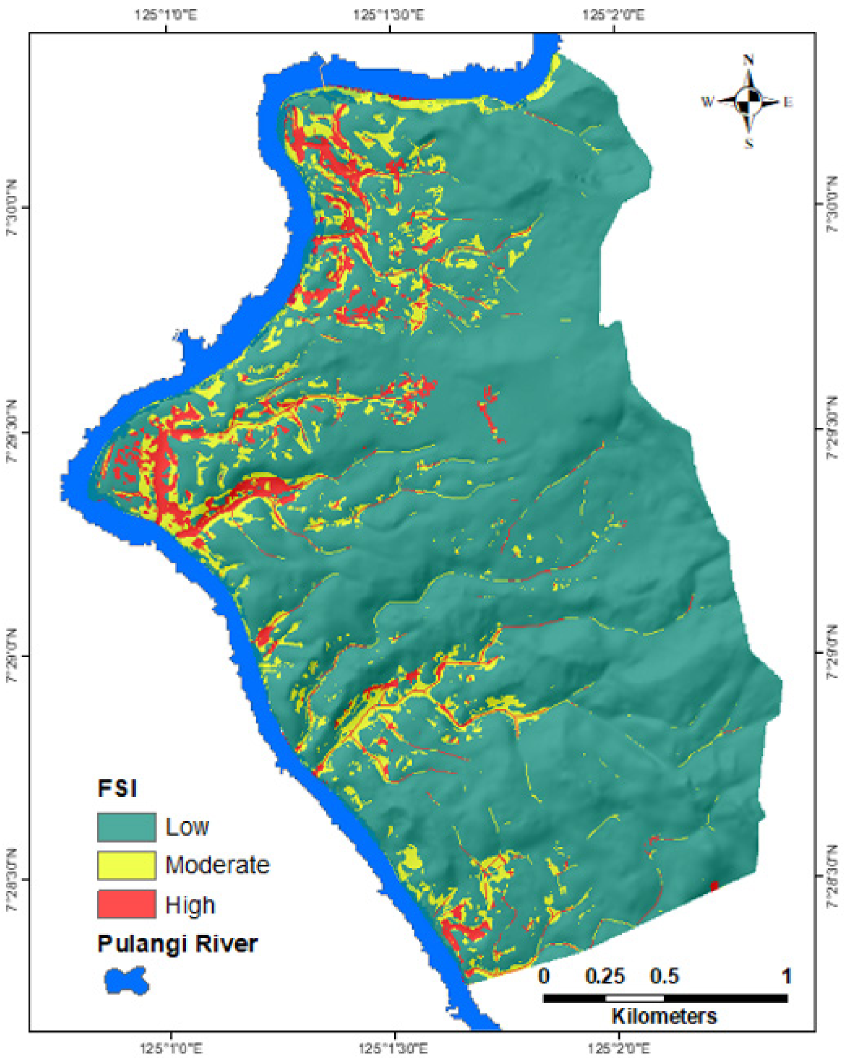

Figure 4. Flashflood susceptibility index map.

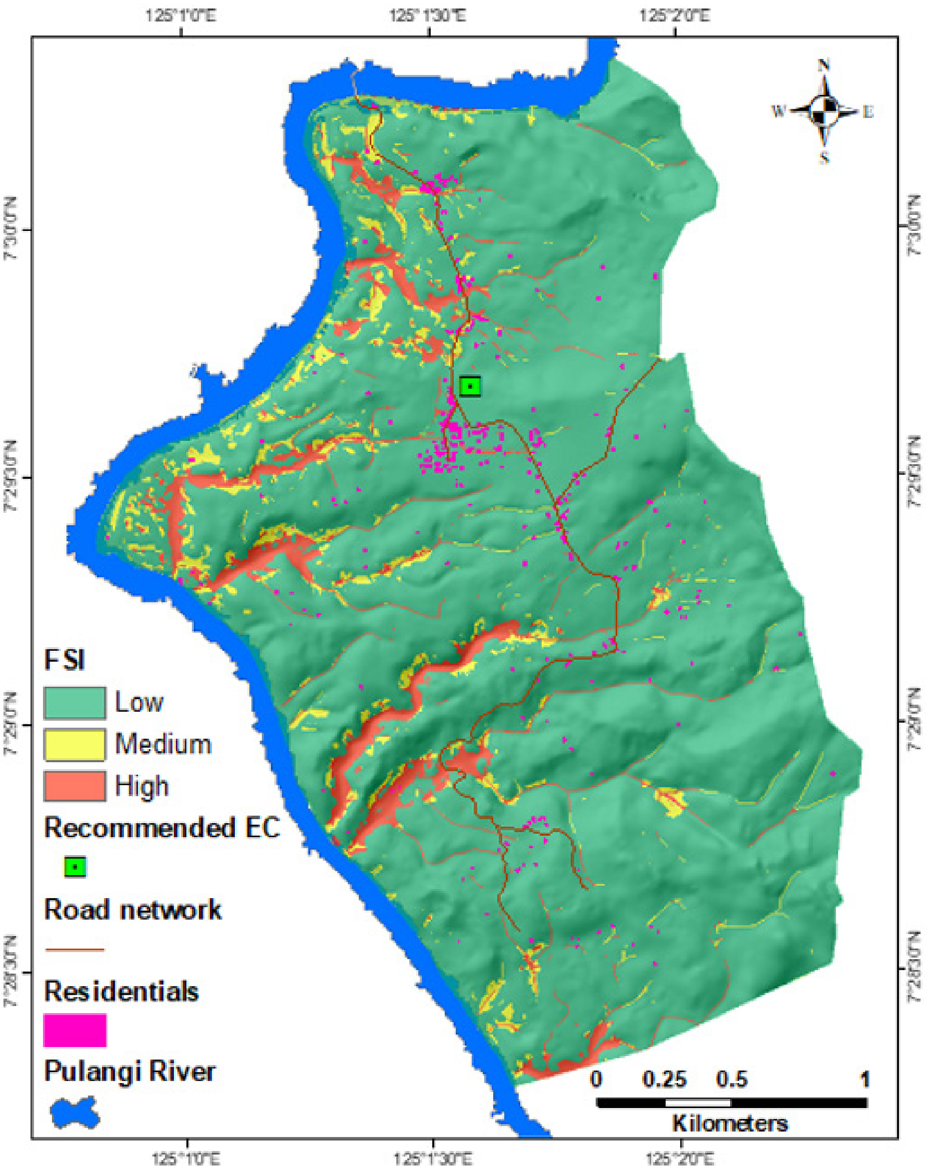

Figure 5. Overlay of FSI and household maps showing the recommended site for evacuation center.

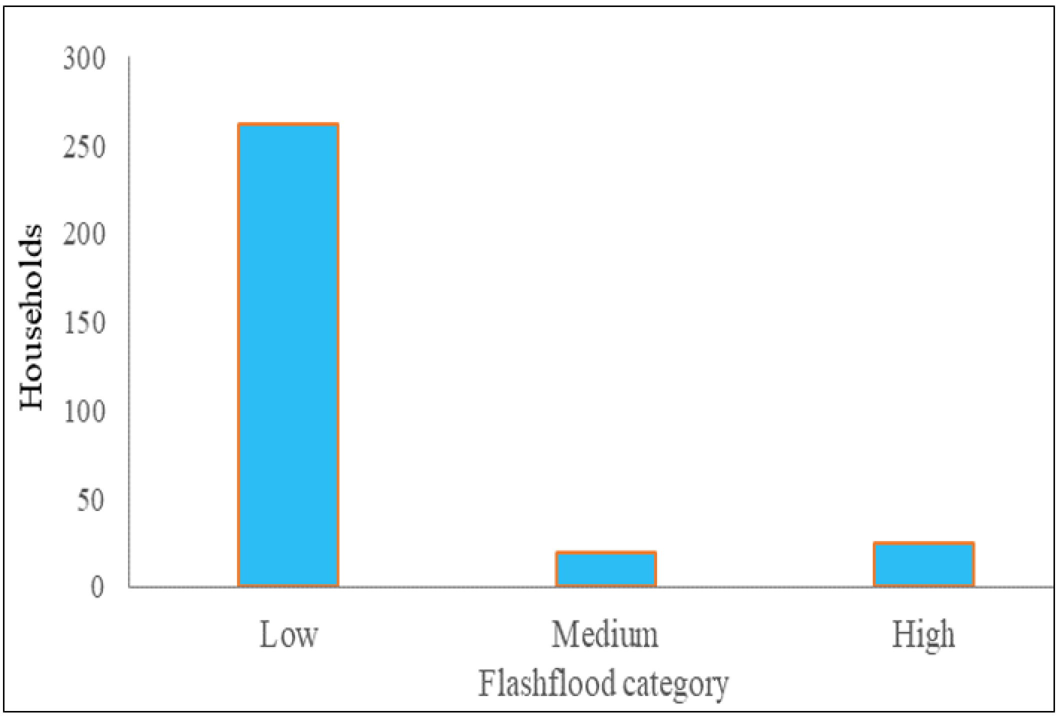

Figure 6. Number of households exposed to flashflood hazards.

around 150 meters above sea level.

CONCLUSION

Flashflood susceptibility index mapping is an essential step for future flood-related hazard management and monitoring. This study enables to assess the status of Bukang Liwayway in terms of flashflood susceptibility as well as determine the number of households that are at high risk of such natural hazards and identify a strategically potential site for an evacuation center. The thematic map layers of the nine controlling factors of flashflood hazards such as elevation, slope, aspect, curvature, topographic wetness index, drainage density, LULC naturalized difference vegetation index, and rainfall were generated following the GIS workflows. Classification of each factor was used as the basis for the relative frequency ratios and the prediction rates calculations. The flash flood susceptibility index map was generated by summing up the relative frequency values and the prediction rates of the nine-factor thematic layers using the raster calculator of the ArcGIS 10.3 application software. The generated flashflood susceptibility index map was classified into low, medium, and high-risk levels. Results show that 89.8, 4.4, and 5.7% of the total land area are at low, medium, and high risk, respectively, with 25 households exposed to high risk and 22 households exposed to medium risk. Further, based on the result of the spatial analysis, the strategic location for a possible evacuation center was identified.

This study's flash flood susceptibility index map can be an essential tool for disaster managers, decision-makers, and engineers in flood risk management plans. Based on the findings of this study, the concerned authorities can adopt appropriate mitigation and preparedness measures to minimize the negative impacts of prevailing and future flood hazards.

ACKNOWLEDGEMENT

This report is a product of the concerted effort of the College of Forestry and Environmental Science research team. The team acknowledges the administration of Central Mindanao University for the funding support, the Research Office for the logistics, and the local government units of Kibawe and Bukang Liwayway for the research opportunities and the full support they provided in the implementation and completion of the project. Above all, to the Almighty Father for the protection and good health.

REFERENCES

Acharya, T.D., & Lee, D.H. (2018). Landslide Susceptibility Mapping using Relative Frequency and Predictor Rate along Araniko Highway. KSCE Journal of Civil Engineering, 23(2019), 763-776. Available online: https://link.springer.com/article/10.1007/s12205-018-0156-x.

Alcantara, J. C. (2019). Overview of the Societal Impacts of Floods in the Philippines. Briefing Note Regional Fellowship Program. https://www.pic.org.kh/images/2019Research/20191014_Overview%20of%20the%20Societal%20Impacts%20of%20the%20Philippines.pdf

Avinash, K.G., & Ashamanjari, K.G. (2010). A GIS and frequency ratio based landslide susceptibility mapping: Aghnashini river catchment, Uttara Kannada, India. International Journal of Geomatics and Geosciences 1(3): 343-354.

Badilla, R. (2008). Flood Modelling in the Pasig-Marikina River. Accessed on 5 October 2014 at http://www.itc.nl/library/papers_2008/msc/wrem/badilla.pdf

Charlton, R., Fealy, R., Moore, S., Sweeney, J., & Murphy, C. (2016). Assessing the impact of climate change on water supply and flood hazard in Ireland using statistical downscaling and hydrological modelling techniques. Climate Change. 74: 475–491. https://doi.org/10.1007/s10584-006-0472-x.

Demir, V., & Kisi, O. (2016). Flood Hazard Mapping by Using Geographic Information System and Hydraulic Model: Mert River, Samsun, Turkey. *Advances in Meteorology*, vol. 2016, 9 pages. https://doi.org/10.1155/2016/4891015

Dingman, S.L. (1981). Elevation: a major influence on the hydrology of New Hampshire and Vermont, USA / L'altitude exerce une influence importante sur l'hydrologie du New Hampshire et du Vermont, Etats-Unis, Hydrological Sciences Journal, 26:4, 399-413. https://doi.org/10.1080/02626668109490904.

Dinesh Kumar, P.K., Gopinath, G., & Seralathan, P. (2007). Application of remote sensing and GIS for the demarcation of groundwater potential zones of a river basin in Kerala, southwest coast of India. Int. J. Remote Sens. 28 (24), 5583–5601.

Forkuo, E.K. (2010). Digital Elevation Modelling Using ASTER Stereo Imagery. Journal of Environmental Science and Engineering, 52(2), pp 81-92.

Kia M.B., Pirasteh, S., Pradhan, B., Mahmud, A.R., Sulaiman, W.N.A,, & Moradi, A. (2012). An artificial neural network model for flood simulation using GIS: Johor River Basin, Malaysia. Environ. Earth Sci. 67: 251–264. https://doi.org/10.1007/s12665-011-1504-z

Lapore, C., Kamal, S.A., Shanahan, P., & Bras, R.L. (2012). Rainfall-induced landslide susceptibility zonation of Puerto Rico. Environ Earth Sci. 66: 1667-1681.

Linham, M., & Nicholls, R.J. (2010). Technologies for Climate Change Adaptation: Coastal erosion and flooding. TNA Guidebook Series. UNEP/GEF.

Lee, S., & Pradhan, B. (2007). Landslide hazard mapping at Selangor, Malaysia using frequency ratio and logistic regression models. Landslides 4 (1), 33–41.

Liuzzo, L., Sammartano, V., & Freni, G. (2019). Comparison between Different Distributed Methods for Flood Susceptibility Mapping. Water Resour Manag. 33: 3155–3173. https://doi.org/10.1007/s11269-019-

02293-w.

Macalalad, R.V., Xu, S., Badilla, R.A., Paat, S.F., Tajones, B.C., Chen, Y., & Bagtasa, G. (2021). Flash flood modeling in the data-poor basin: A case study in Matina River Basin. Tropical Cyclone Research and Review 10(2021), 87-95. Accessed: Nov. 4, 2021. https://www.sciencedirect.com/journal/tropical-cyclone-research-and-review.

Manap, M.A., Nampak, H., Pradhan, B., Lee, S., Sulaiman, W.N.A., & Ramli, M.F. (2014). Application of probabilistic-based frequency ratio model in groundwater potential mapping using remote sensing data and GIS. Arab. J. Geosci. 7 (2), 711–724

McDougall, K., Liu, x., Basnet, B., & Apan, A. (2008). “Evaluation of current DEM Accuracy for Condamine Catchment”, Proceedings of the 8th International Symposium on Spatial Accuracy Assessment in Natural Resources and Environmental Sciences Shanghai, P. R. China, June 25-27, 2008, pp 71-78.

Nguyen, B., Minh, D., Ahmad, A., & Nguyen, Q. (2020). The role of relative slope length in flood hazard mapping using AHP and GIS: A case study: Lam River Basin, Vietnam. *Geography, Environment, Sustainability. 13*(2):115-123. https://doi.org/10.24057/2071-9388-2020-48

Paul, GC, Saha S, & Hembram TK. (2019). Application of the GIS-Based Probabilistic Models for Mapping the Flood Susceptibility in Bansloi Sub-basin of Ganga-Bhagirathi River and Their Comparison. Remote Sens Earth Syst Sci. 2: 120–146. https://doi.org/10.1007/s41976-019-00018-6.

Puno, G.R., Puno, R.C.C., & Maghuyop, I.V. (2021). Two-dimensional flood model for risk exposure analysis of land use/land cover in a watershed. Global Journal of Environmental Science and Management, 7(2): 225-238.

Samantha, R.K., Bhunia, G.S., Shit, P.K., & Pourghasemi, H.R. (2018). Flood susceptibility mapping using geospatial frequency ratio technique: a case study of Subarnarekha River Basin, India. Model Earth Syst Environ., 4: 395–408. https://doi.org/10.1007/s40808-018-0427-z

Sangeeta, & Maheshwari, B.K. (2018). Earthquake-Induced Landslide Hazard Assessment of Chamoli District, Uttarakhand Using Relative Frequency Ratio Method. Indian Geotech J. 49, 108-123. https://doi.org/10.1007/s40098-018-0334-2

Tehrany, M.S., Shabani, F., Jebur, M.N., Hong, H., Chen, W., & Xie, X. (2017). GIS-based spatial prediction of flood prone areas using standalone frequency ratio, logistic regression, weight of evidence and their ensemble techniques. Geomatics, Natural Hazards and Risk, 8(2); 1538-1561. https://doi.org/10.1080/19475705.2017.1362038

Tran, P., Shaw, R., Chantry, G., & Norton, J. (2009). GIS and Local Knowledge is Disaster Management: A Case Study of Flood Risk Mapping in Viet Nam. Disasters 33(1): 152-169. https://pubmed.ncbi.nlm.nih.gov/18513310/

Ullah, K., & Zhang, J. (2020). GIS-based flood hazard mapping using relative frequency ratio method: A case study of Panjkora River Basin, esaern Hindu Kush, Pakistan. Plos One. 15(3): e0229153. https://doi.org/10.1371/journal.pone.0229153

UNDRR (2019). Disaster Risk Reduction in the Philippines: Status Report 2019. Bangkok, Thailand, United Nations Office for Disaster Risk Reduction (UNDRR), Regional Office for Asia and the Pacific

Wu, Y., Li, W., Wang, Q., & Yan, S. (2016). Landslide susceptibility assessment using frequency ratio, statistical index and certainty factor models for the Gangu County, China. Arabian Journal of Geosciences, 9(2), 84 p.

Zhang, D., Quan, J., Zhang, H., Wang, F., Wang, H., & He, X. (2015). Flash flood hazard mapping: a pilot case study in Xiapu River Basin, China. Water Science and Engineering 8 (3), 195-204.

Zhang, G., Cai, Y., Zheng, Z., Zhen, J., Liu, Y., & Huang, K. (2016). Integration of the statistical index method and the analytic hierarchy process technique for the assessment of landslide susceptibility in Huizhou, China. CATENA, Vol. 142, No. Supplement C, pp. 233-244, DOI: 10.1016/j.catena.2016.03.028.

ZURICH (2020). Three common types of flood explained. Accessed: Nov. 4, 2021.